



**HAL**  
open science

## On potential CBOC/TMBOC common receiver architectures

Olivier Julien, Christophe Macabiau, Jose-Angel Avila-Rodriguez, Stefan Wallner, Matteo Paonni, Günter Hein, Jean-Luc Issler, Lionel Ries

► **To cite this version:**

Olivier Julien, Christophe Macabiau, Jose-Angel Avila-Rodriguez, Stefan Wallner, Matteo Paonni, et al.. On potential CBOC/TMBOC common receiver architectures. ION GNSS 2007, 20th International Technical Meeting of the Satellite Division of The Institute of Navigation, Sep 2007, Fort Worth, United States. pp 1530 - 1542. hal-01022131

**HAL Id: hal-01022131**

**<https://enac.hal.science/hal-01022131>**

Submitted on 20 Nov 2014

**HAL** is a multi-disciplinary open access archive for the deposit and dissemination of scientific research documents, whether they are published or not. The documents may come from teaching and research institutions in France or abroad, or from public or private research centers.

L'archive ouverte pluridisciplinaire **HAL**, est destinée au dépôt et à la diffusion de documents scientifiques de niveau recherche, publiés ou non, émanant des établissements d'enseignement et de recherche français ou étrangers, des laboratoires publics ou privés.

# On Potential CBOC/TMBOC Common Receiver Architectures

O. Julien, C. Macabiau

*Ecole Nationale de l'Aviation Civile (ENAC), France*

J.-A. Avila Rodriguez, S. Wallner, M. Paonni, G. W. Hein  
*University FAF Munich, Germany*

J.-L. Issler, L. Ries

*Centre Nationale d'Etude Spatiales (CNES), France*

## BIOGRAPHIES

**Olivier Julien** is an assistant professor at the signal processing laboratory of ENAC (Ecole Nationale de l'Aviation Civile), Toulouse, France. His research interests are GNSS receiver design, GNSS multipath and interference mitigation and GNSS interoperability. He received his B.Eng in 2001 in digital communications from ENAC and his PhD in 2005 from the Department of Geomatics Engineering of the University of Calgary, Canada.

**José-Ángel Ávila-Rodríguez** is research associate at the Institute of Geodesy and Navigation at the University of the Federal Armed Forces Munich. He is responsible for research activities on GNSS signals, including BOC, BCS, and MBOC modulations. Avila-Rodríguez is one of the CBOC inventors and has actively participated in the developing innovations of the CBOC multiplexing. He is involved in the GALILEO program, in which he supports the European Space Agency, the European Commission, and the European GNSS Supervisor Authority, through the GALILEO Signal Task Force.

**Christophe Macabiau** graduated as an electronics engineer in 1992 from the ENAC (Ecole Nationale de l'Aviation Civile) in Toulouse, France. Since 1994, he has been working on the application of satellite navigation techniques to civil aviation. He received his Ph.D. in 1997 and has been in charge of the signal processing lab of the ENAC since 2000.

**Stefan Wallner** studied at the Technical University of Munich and graduated in 2003 with a Diploma in Techno-Mathematics. He is now research associate at the Institute of Geodesy and Navigation at the University of the Federal Armed Forces Germany in Munich. His main topics of interests can be denoted as the Spreading Codes, the Signal Structure of GALILEO together with Radio Frequency Compatibility of GNSS.

**Matteo Paonni** is research associate at the Institute of Geodesy and Navigation at the University of the Federal Armed Forces Munich. He received his M.S. in Electrical Engineering from the University of Perugia, Italy. His main topics of interests are Tracking Algorithms for

GNSS Receiver Design, GNSS Signal Structure and Indoor Positioning.

**Guenter W. Hein** is Full Professor and Director of the Institute of Geodesy and Navigation at the University FAF Munich. He is responsible for research and teaching in the fields of high-precision GNSS positioning and navigation, physical geodesy and satellite methods. He has been working in the field of GPS since 1984 and is author of numerous papers on kinematic positioning and navigation as well as sensor integration. In 2002 he received the prestigious "Johannes Kepler Award" from the US Institute of Navigation (ION) for "sustained and significant contributions to satellite navigation". Presently he is heavily involved in the Galileo program.

**Jean-Luc Issler** is head of the Transmission Techniques and signal processing department of CNES, whose main tasks are signal processing, air interfaces and equipments in Radionavigation, TT&C, propagation and spectrum survey. He is involved in the development of several spaceborne receivers in Europe, as well as in studies on the European RadioNavigation projects, like GALILEO and the Pseudolite Network. With DRAST, he represents France in the GALILEO Signal Task Force of the European Commission. With Lionel Ries and Laurent Lestarquit, he received in 2004 the Astronautic Prize of the AAAF ( French aeronautical and space association ) for his technical work on GALILEO signals and spaceborne GNSS equipments.

**Lionel Ries** is a navigation engineer in the Transmission Techniques and signal processing department, at CNES since June 2000. He is responsible of research activities on GNSS2 signal, including BOC modulations and GPS IIF L5. He is involved in the GALILEO program, in which he supports ESA, EC and GJU, through the GALILEO Signal Task Force. He graduated in 1997 from the Ecole Polytechnique de Bruxelles, at Brussels Free University, Belgium, in 1997, and received a M.S. degree from the Ecole Nationale Supérieure de l'Aéronautique et de l'Espace in Toulouse, France, in 1998.

## ABSTRACT

Under the 2004 *Agreement on the Promotion, Provision, and Use of Galileo and GPS Satellite-Based Navigation Systems and Related Applications*, the member states of the European Union and the United States agreed on working together, intensifying thus the cooperation on interoperability and compatibility issues between Galileo and GPS. Among other topics, one important focus was the E1/L1 frequency band, centred at 1575.42 MHz, where the Galileo E1 Open Service (OS) signal and the modernized GPS L1 civil (L1C) signal are going to be transmitted along with many other RNSS signals. Recent efforts made by US and European experts identified a common optimized Power Spectral Density (PSD) frame, known as Multiplexed BOC (MBOC), in which both the Galileo E1 OS and the GPS L1C signals would fit. This normalized MBOC PSD is actually formed by the sum of 10/11 of the normalized BOC(1,1) PSD and 1/11 of the normalized BOC(6,1) PSD. Because the MBOC is defined in the frequency domain, the time representation cannot be uniquely defined, and at least two different implementations that would still comply with the MBOC spectrum exist: CBOC and TMBOC. Indeed, the latest developments indicate that the main Galileo E1 OS and GPS L1C candidates will exhibit different features [3],[4]:

- The current GPS L1C main candidate will have a pure BOC(1,1) data channel gathering 25% of the total signal power while the pilot channel will use a Time-Multiplexed BOC (TMBOC) modulation with 75% of the total civil signal power..
- The current Galileo E1 OS main candidate will equally share its power between its data and pilot channels, with the important difference with respect to TMBOC that in both channels a Composite BOC (CBOC) modulation with BOC(6,1) will be used.

It is well-understood that the definition of a common PSD for the GPS and Galileo civil signals on E1/L1 calls for an increased interoperability and compatibility of these signals at the user level. However, to really promote the use of GPS/Galileo E1/L1 combined receivers, it is of greatest importance to find GPS L1C and Galileo E1 OS tracking architectures that minimize the receiver complexity while maintaining high quality measurements. This is particularly true since the main candidates for implementation of MBOC for GPS L1C and Galileo E1 OS are already baseline of their respective systems [3].

The purpose of this article is to thoroughly investigate possible GPS/Galileo receiver architectures that could be adapted to CBOC, TMBOC or both waveforms and to assess their performance. The first step of the proposed analysis is to assess the interference that both GPS and Galileo signals will cause on each other. This step is necessary in order to evaluate the degradation that Galileo and GPS signals will cause on each other, and thus, to

assess precisely the quality of the forthcoming tracking loops. In a second part, several CBOC/TMBOC tracking architectures meant to minimize the complexity of a combined GPS/Galileo receiver will be presented and their performances in terms of resistance to thermal noise and multipath, as well as their complexity, will be compared to optimal architectures dedicated to CBOC-only or TMBOC-only receivers. This part aims at giving an insight on which key parameters can be modified to find a relevant trade-off between receiver complexity and performance for the general user. Finally, in the last section, different multipath mitigation techniques will be tested according to different receiver configurations – BOC(1,1) or MBOC receiver – and flexibility in the number of correlators available for each channel – pilot or data + pilot tracking. In particular, innovative multipath mitigation techniques based on a multi-correlator receiver are also investigated.

## INTRODUCTION

After a long period of discussions, the Galileo Signal Plan has finally been frozen with the definitive decision of both GPS and Galileo to implement the MBOC (Multiplexed BOC) modulation for the Galileo E1 Open Service (OS) and the GPS L1 Civil (L1C) Signal in E1/L1 ([1], [2] and [3]). While the baseline of the rest of Galileo signals in E5 and E6 has been relatively stable along the past years, the E1/L1 band has been in continuous evolution. The most important reason for this is the severe degree of congestion that the E1/L1 band presents.

MBOC(6,1,1/11) is the result of the desire to multiplex a wideband signal – the BOC(6,1) – with a narrow-band signal – the BOC(1,1) – in such a way that 1/11 of the power is allocated in average on the BOC(6,1) component [5]. The MBOC normalized Power Spectral Density (PSD) of the data and pilot components together, specified without the effect of band-limiting filters and payload imperfections, is given by

$$G_{MBOC(6,1,1/11)}(f) = \frac{10}{11} G_{BOC(1,1)}(f) + \frac{1}{11} G_{BOC(6,1)}(f) \quad (1)$$

Figure 1 shows all the existing and planned navigation signals of the four global navigation systems that are foreseen to play an important role in the future [4]. It can be seen that the MBOC succeeds in minimizing its overlap with other navigation signals in the E1/L1 band. Moreover, it also fulfills very well the requirements of mass-market users as it provides a signal with a narrow-band component where most of the power is allocated. At the same time, MBOC also has a wide band component that is meant to provide future users with an additional potential to improve performance.

As shown in [5], a variety of time waveforms can be used to produce the MBOC(6,1,1/11) PSD. Two fundamentally

different approaches, the Time-Multiplexed BOC (TMBOC) and the Composite BOC (CBOC) have been selected for the MBOC implementation of GPS and Galileo respectively. These are described in the next section

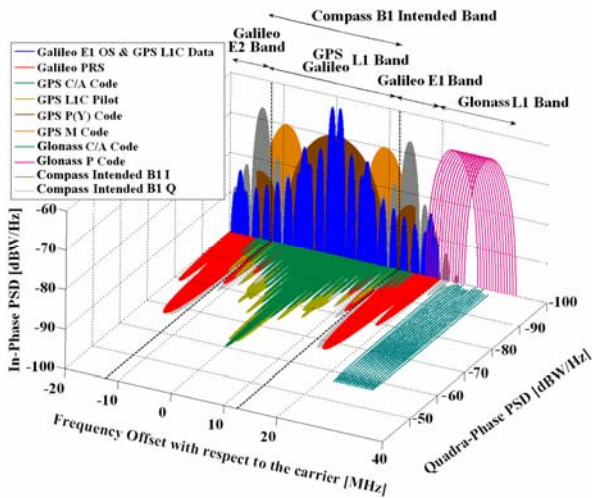


Figure 1. Spectra of GPS, Galileo, GLONASS and Compass Intended Signals in E1/L1 [4]

## PRESENTATION OF GALILEO E1 OS AND GPS L1C WAVEFORMS

### The Galileo E1 OS Signal

The Galileo E1 Open Service (OS) will use a CBOC (Composite Binary Offset Carrier) modulation to implement the MBOC. The CBOC signal adopted for Galileo is based on the approach presented in [3], [4], [5] and [6], using a four-level sub-carrier formed by the weighted sum of BOC(1,1) and BOC(6,1) symbols on both data and pilot. The CBOC modulation is a particular case of the CBCS multiplexing scheme that was presented in [6] where the particular BCS sequence is in this case a BOC(6,1). Therefore, all the theory derived in [4] and [6] is also valid here to describe the CBOC case and one only has to substitute in the equations the generic BCS case by the particular BOC(6,1) sequence and the power of 1/11.

The normalized base-band Galileo E1 OS composite signal model is given by:

$$s_{E1}(t) = \frac{1}{\sqrt{2}} \begin{Bmatrix} e_{E1-B}(t)d_{E1-B}(t)[Px(t)+Qy(t)] \\ -e_{E1-C}(t)[Px(t)-Qy(t)] \end{Bmatrix} \quad (2)$$

where

- $e_{E1-B}(t)$  and  $e_{E1-C}(t)$  are the data and pilot spreading sequences respectively,
- $d_{E1-B}(t)$  is the Galileo E1-B navigation message, and
- $x$  and  $y$  are the sine-BOC(1,1) and sine-BOC(6,1) sub-carriers respectively.

It can be noted that both pilot and data components are modulated onto the same carrier component, with a power split of 50 percent.

The parameters  $P$  and  $Q$  are chosen such that the power associated with the BOC(6,1) sub-carrier components equals 1/11 of the total power of the whole Galileo E1 OS signal (data + pilot). This yields:

$$P = \sqrt{\frac{10}{11}} \quad Q = \sqrt{\frac{1}{11}} \quad (3)$$

Figure 2 shows a generic view of the Galileo E1 OS generation scheme.

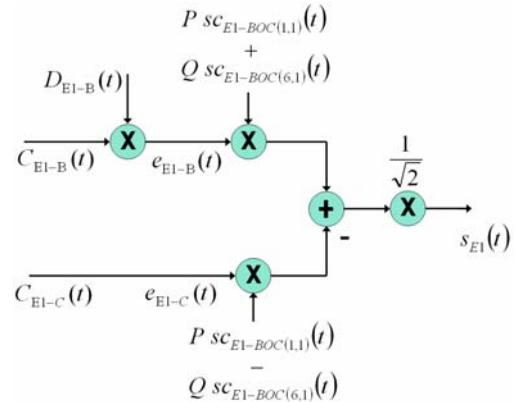


Figure 2. Modulation Scheme of Galileo E1 Signals

If we take a careful look at equation (2), it can be recognized that the CBOC modulation has the data and pilot sub-carriers in anti-phase (with respect to the BOC(6,1) component). This can be observed on the equivalent waveform of each channel, shown in Figure 3.

As it was already mentioned in [4], [5], [13], and [16], and as a result of the slight differences in the data and pilot CBOC sub-carriers, slight differences are also observed in the relative performances of the data and pilot channels, especially for wide-band receivers. These differences favour indeed the performance of the pilot channel where BOC(1,1) and BOC(6,1) are subtracted.

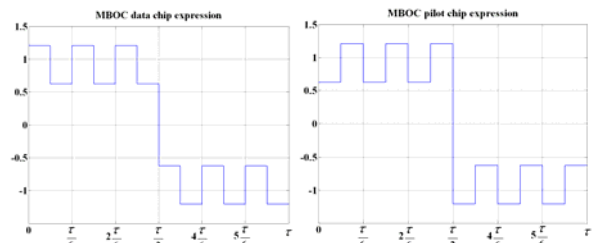


Figure 3. Data (Left) and Pilot (Right) CBOC Sub-Carriers

### The GPS L1C Signal

TMBOC is the selected MBOC implementation of GPS [7] and is characterized by using a binary sub-carrier component that results from the time-multiplexing of the

BOC(1,1) and BOC(6,1) sub-carriers according to a deterministic pattern. The GPS L1C base-band signal can be written as:

$$s_{L1C}(t) = \frac{1}{\sqrt{2}} \left\{ \begin{array}{l} e_{L1C-I}(t) d_{L1C-I}(t) x(t) \\ + e_{L1C-Q}(t) TMBOC(6,1,4/33) \end{array} \right\} \quad (4)$$

where

- $TMBOC(6,1,p)(t) = \begin{cases} x(t) & \text{if } t \in S_1 \\ y(t) & \text{if } t \in S_2 \end{cases}$
- $S_1$  is the union of the segments of time when a BOC(1,1) sub-carrier is used, while  $S_2$ , the complement of  $S_1$  in the time domain, is the union of the segments of time when a BOC(6,1) sub-carrier is used.

Figure 4 shows a generic view of a TMBOC modulation time series. Additionally, all the data channel is exclusively modulated by a BOC(1,1) sub-carrier, while the pilot channel is modulated by a TMBOC sub-carrier, where 29/33 chips of the spreading code are modulated by a BOC(1,1) sub-carrier and the remaining 4/33 chip are modulated by a BOC(6,1) sub-carrier. It is important to note that although all the BOC(6,1) sub-carrier is on the pilot channel, the average power is shown to fulfil Equation (1).

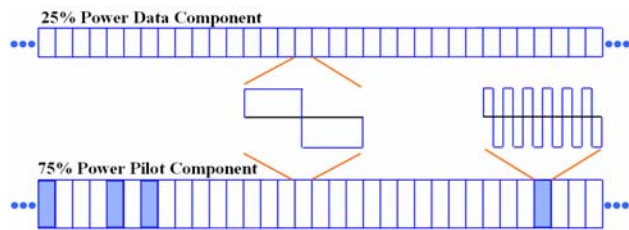


**Figure 4. Example of TMBOC(6,1,4/33) Spreading Time Series, with all BOC(6,1) Spreading Symbols in the 75% Pilot Power Component**

The exact locations of the BOC(6,1) spreading symbols obeys a rationale as shown in [3] and [8]. In fact, if the BOC(6,1) symbols are properly placed, the spreading codes' auto and cross-correlation can be further improved. As seen in equation (4), the selected GPS implementation of TMBOC places 75% of the total power on the pilot channel while the other 25% is reserved for data.

### CBOC and TMBOC, Same Spectrum, Different Signals

During the optimization of the E1/L1 Galileo and GPS signals, special care was put on designing a common signal structure, from a spectrum point of view, from which both GPS and Galileo could profit the most. The main idea behind was that in the future receivers will not only receive GPS or Galileo alone but will try to use both to exploit the geometry improvement brought by a dual constellation. The first step towards that is obviously that

the receiver should be capable of processing both Galileo E1 OS and GPS L1C signals together.

As we have seen in previous sections, Galileo E1 OS and GPS L1C are very similar signals in the sense that they have the same PSD and it has been shown that in average they perform the same. However, the CBOC and TMBOC modulations are quite different and an optimum combined receiver should account for the differences between both.

CBOC is a four-level signal with data and pilot in anti-phase. In addition, the power split between data and pilot is of 50/50 and both data and pilot have a narrow BOC(1,1) and a wide-band BOC(6,1) component with the same power. On the contrary, TMBOC is a binary signal with a data narrow-band channel consisting of only BOC(1,1) symbols while the pilot channel contains all the wide-band BOC(6,1) component of the signal. Moreover, 75% of the total power concentrates on the pilot channel while only 25% is allocated to the data channel. Two signals, one spectrum, two different concepts.

When considering future combined GPS/Galileo receivers, the first step is to investigate how both signals can interfere with each other and if this can be detrimental for the signal processing part. This is done in the next section

### ASSESSMENT OF CBOC/TMBOC SELF-INTERFERENCE

The main objective of this section is to show the degradation that a Galileo or GPS receiver is theoretically expected to suffer when other Galileo and GPS signals interfere with the useful signal. In order to measure this effect, the equivalent increase of the noise floor due to non-desired signals will be investigated at the prompt correlator output. It is well known that the equivalent noise floor at the correlator input when an interferer is present is the sum of:

- the thermal noise floor, and
- an additional noise floor that creates the same error variance at the correlator output as the interferer.

In the present case, the interference can be due to the same system as is the situation of that interference coming from the desired signal (intra-system interference) or due to a different system (inter-system interference). Thus:

$$(N_0)_{eff} = N_0 + I_{INTRA} + I_{INTER} \quad (5)$$

The intra- and inter-system interference depends on the power of the interfering signals and a well known figure called Spectral Separation Coefficient (SSC).  $I_{INTRA}$  can generally be defined as [12]:

$$I_{INTRA} = \frac{\sum_{j=1}^{N_{INTRA}} C_j \kappa_{js}}{\int_{-\beta_r/2}^{\beta_r/2} G_s(f + f_{dop_s}) df} \quad (6)$$

where

- $N_{INTRA}$  is the number of received signals belonging to the same system as the desired one,
- $C_j$  is the received power of signal  $j$ ,
- $\beta_r$  is the receiver front-end-bandwidth,
- $\beta_t$  is the transmitter front-end-bandwidth,
- $G_s(f)$  is the PSD of the desired signal  $s$ ,
- $f_{dop_s}$  is the Doppler frequency offset of the desired signal  $s$ ,
- $\kappa_{js}$  is the SSC between signal  $j$  and the desired signal  $s$ ,
- $G_j$  is the PSD of the non desired signal  $j$ , and
- $f_{dop_j}$  is the Doppler frequency offset of the non desired signal  $j$

The computation of the equivalent noise power density  $I_{INTER}$  is identical to  $I_{INTRA}$  in (6) with the only exception that the summation in the numerator has to be done for all signals that do not belong to the desired signal's system.

Due to the increasing number of GNSS satellites and thus signals, the inter- and intra-system interference has to be assessed thoroughly in order to make sure that it does not harm the acquisition and tracking operations. In particular, it is important to control that certain common assumptions used for the computation of the SSCs, such as the infinite spreading code length, are usable in order to minimize the risk of unforeseen interoperability problems.

### Computation of SSCs via simulations

A generic model to compute the SSC, representing the typical correlation operation, is given in Figure 5. It must be noted that the input signal before the correlation is normalized to 1W of power according to (6). If the only interference is an Additive White Gaussian Noise (AWGN), and the front-end filter is assumed rectangular, the PSD of the product between the incoming signal and the reference signal is equal to:

$$G_1(f) = N_0 \int_{-\infty}^{+\infty} \text{rect}\left(\frac{u}{\beta_r}\right) G_s(u-f) du = N_0 \int_{-\beta_r/2}^{\beta_r/2} G_s(u-f) du \quad (7)$$

where  $N_0$  represents the noise floor.

This PSD has a frequency occupancy significantly large compared to the I&D filter bandwidth. Consequently, the PSD of the correlator output can be approximated by:

$$G_2(f) \approx G_1(0) |H_{ID}(f)|^2 = N_0 |H_{ID}(f)|^2 \int_{-\beta_r/2}^{\beta_r/2} G_s(f) df \quad (8)$$

where  $H_{ID}(f)$  is the Integrate and Dump filter.

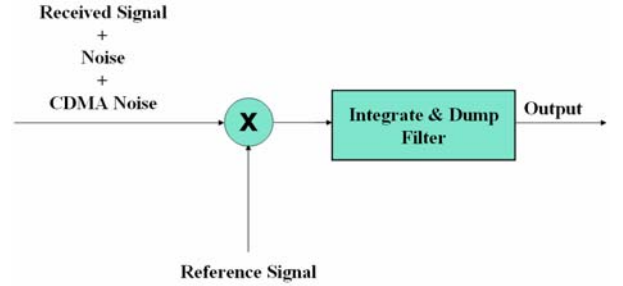


**Figure 5. SSC Model to measure the increase of noise floor due to CDMA noise from other non-desired signals**

The correlator output noise variance will then be:

$$\sigma^2 \approx \int_{-\infty}^{+\infty} G_2(f) df = \frac{N_0}{T} \int_{-\beta_r/2}^{\beta_r/2} G_s(f) df \quad (9)$$

where  $T$  is the coherent integration of the interfering signal and the replica.

But a more interesting case is that of non-white interference. Then, the variance of the correlator output noise is shown to be:

$$\sigma^2 = \int_{-\infty}^{+\infty} \int_{-\beta_r/2}^{\beta_r/2} G_k(u) G_s(u-f_1) du |H_{ID}(f_1)|^2 df_1 \quad (10)$$

Assuming that the multiplier output PSD is sufficiently flat across the I&D filter, which is true when a very long pseudorandom noise code is employed, the assumption of flatness of  $\int_{-\infty}^{+\infty} G_k(u) G_s(u-f_1) du$  can be used as it was done for the AWGN case. The SSC is then shown to be approximated by the following expression:

$$\kappa_{ks} \approx \frac{\int_{-\beta_r/2}^{\beta_r/2} G_k(f) G_s(f) df}{\int_{-\beta_r/2}^{\beta_r/2} G_s(f) df} \quad (11)$$

While this is true for very long codes, it has been shown in the literature ([8], [9], [10] and [11]) that for shorter codes important differences can be observed between the ideal flat SSC and that measured at the receiver. Indeed, it is well known that the PSD of CDMA signals using short codes is a line spectrum and thus cannot be considered as smoothed. In this case, the SSC can only be expressed as:



$$\kappa_{ks} \approx \frac{\int_{-\infty}^{\infty} \int_{-\beta_r/2}^{\beta_r/2} G_k(u) G_s(u - f_1) du |H_{ID}(f_1)|^2 df_1}{\int_{-\beta_r/2}^{\beta_r/2} G_s(f) df} \quad (12)$$

However, this expression is very difficult to assess. The most extreme case is that of the C/A code where due to its short code nature and its 20 repetitions within a data bit, the SSC can raise by nearly 12 dB in the worst case. It is then necessary to assess the SSCs values between GPS and Galileo MBOC signals through a series of tests that model exactly the correlator output model shown in Figure 5 using the true GPS and Galileo spreading codes.

### SSC Degradation of CBOC and TBOC receivers using simulations

It is obvious that the value of the equivalent noise floor will depend upon the power of each interferer. Thus it is of great importance to choose a scenario representing a worst case with the greatest fidelity. That was done using the configuration of Table 1 for the interfering and desired signals. It represents a situation where the interfering signals (of the same system or from other systems) are raising the noise floor to the maximum level with respect to the power of the desired signal. In addition, it is also assumed to be representative of a situation where the spectral separation coefficients will also be worst case. However it must be noted that the increase in noise floor does not always correspond to the case where the SSC adopts its worst case, but could also be due to the high interfering power at that specific location and moment in the time.

**Table 1. Parameters of the SSC Simulations**

Interfering Signals			
PRN	Doppler [Hz]	Delay [ms]	Power [dBW]
31	+170.68	73.84	-155.39
30	-751.33	71.25	-153.43
5	+2993.33	75.58	-155.76
6	+3286.90	77.00	-155.69
2	+1232.49	71.26	-153.42
4	-1498.58	72.13	-154.26
20	-3246.60	80.59	-157.86
23	+1567.92	76.16	-155.52
Desired Signal			
13	+3258.75	81.18	-158.62

It must be noted that the results would not differ significantly if other PRN codes were considered and therefore the results can be considered as representative of a typical worst case scenario.

It is well known that phase tracking is less robust than code tracking. Consequently, it would be interesting to investigate the correlator output noise characteristics that would correspond to that used by the PLL. Two different

families of receivers are considered herein that correspond to classical receiver configurations to receive an MBOC signal:

- TBOC or CBOC receivers optimized for both signal waveforms, and
- BOC(1,1) receivers.

In order to simplify the number of simulations, only the Galileo E1 data channel is considered. Simulations have shown that the inter and intra-system interference degradation due to the Galileo E1 OS pilot channel is comparable to that due to the data channel since the spectrum is also very similar. Thus in the following, CBOC will refer to the CBOC data signal only.

For both receiver configurations, the same simulated strategy was employed. It follows a linear approach and the correlator output was assessed for all possible code phase offsets between the interfering normalized signal and the ideal replica in steps of 1/12 chips. That means that for the case of a Galileo receiver 4092x12 different code offsets flow into the statistic while for GPS we will have 10230x12 samples.

Moreover, for all the simulations a dwell time of 20 ms was used for the receiver. This corresponds to the typical PLL integration time. Indeed, due to the receiver clock instability, the correlator that will feed the PLL discriminator will likely not use a very long integration. It seems that 20 ms, already used for GPS C/A, is a good duration. This means in other words that assuming a desired Galileo signal, the considered output is the sum of 5 times 4 ms coherent integrations since the primary Galileo E1 OS code duration is 4 ms. In the same manner, since the length of the GPS L1C primary code is of 10 ms, the considered output will consist of two samples resulting from a coherent integration of 10 ms.

Figure 6 shows the output of a CBOC correlator when the interfering signals are

- the data channel of Galileo E1 OS with its corresponding codes, or
- the data channel of Galileo E1 OS spread with “random” codes.

As it can be observed, the Galileo E1 OS codes deliver values slightly higher than those of an ideal random code, proving the interest of this analysis.

Table 2 summarizes the results of all the analyzed cases (12 samples were used for each test case). As it can be seen, the SSCs obtained using the true Galileo and GPS codes are very similar (within 0.5 dBs) to the theoretical and simulated ones assuming a smooth PSD. An explanation for this is the fact that the data bits (or the secondary codes if the pilot channel is concerned) help in

making the spreading code “look longer”, and thus more random. It can be concluded from the simulations that the TmBOC and CBOC implementations of MBOC, in spite of being slightly different, will not interfere with each other significantly, and more importantly, can be very well approximated by the smooth spectrum approach.

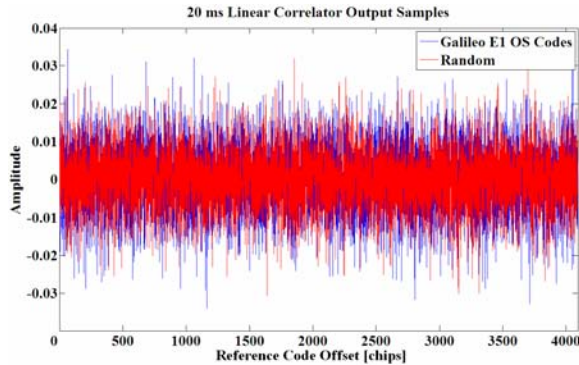


**Figure 6. 20 ms CBOC Correlator Output Amplitude assuming an interferer formed by CBOC signals modulated with random and Galileo E1 OS codes**

Furthermore, the introduced additional degradation with respect to ideal spectrum SSC is measured by the following parameter:

$$\Delta\sigma_{RND}^{CDMA} = \left( \frac{\sigma_{CDMA}}{\sigma_{RND}} \right)^2 \quad (13)$$

As it can be seen in Table 2, this parameter is always lower than 0.5 dB and indeed falls within the accuracy of the realized simulations. In addition, it is also expected that more accurate simulations will further reduce the relative increase of the SSC.

Since it has been shown that there was no major unforeseen threat from the GPS/Galileo self-interference,

**Table 2. Derived Spectral Separation Coefficients for different receiver and interference configurations. BOC refers to BOC(1,1) and CBOC to the data in-phase component.**

Interfering System and Signals		Desired System and Signals		$\sigma_{CDMA}$	$\sigma_{RND}$	$\Delta\sigma_{RND}^{CDMA}$	$SSC_{CDMA}$	$SSC_{RND}$	Ideal SSC
Galileo	CBOC	Galileo	CBOC	0.0088	0.0083	0.4671	-65.1	-65.6	-65.32
GPS	BOC	Galileo	BOC	0.0092	0.0088	0.4394	-64.7	-65.1	-64.87
GPS	TmBOC	Galileo	CBOC	0.0085	0.0081	0.4173	-65.4	-65.8	-65.63
Galileo	CBOC	Galileo	BOC	0.0089	0.0085	0.4549	-64.9	-65.4	-65.11
Galileo	CBOC	GPS	BOC	0.0056	0.0055	0.2673	-65.0	-65.2	-65.11
GPS	TmBOC	Galileo	BOC	0.0087	0.0083	0.4017	-65.2	-65.6	-65.42
Galileo	BOC	GPS	BOC	0.0058	0.0056	0.2523	-64.7	-65.0	-64.87
GPS	TmBOC	GPS	BOC	0.0055	0.0053	0.2437	-65.2	-65.5	-65.42
GPS	TmBOC	GPS	TmBOC	0.0052	0.0051	0.2697	-65.6	-65.9	-65.92
Galileo	CBOC	GPS	TmBOC	0.0054	0.0052	0.3115	-65.4	-65.7	-65.63
Galileo	BOC	Galileo	BOC	0.0092	0.0087	0.4577	-64.7	-65.2	-64.87
GPS	BOC	GPS	BOC	0.0058	0.0057	0.2616	-64.7	-65.0	-64.87
GPS	BOC	Galileo	CBOC	0.0090	0.0085	0.4596	-64.9	-65.4	-65.11
GPS	BOC	GPS	TmBOC	0.0055	0.0053	0.2915	-65.2	-65.5	-65.42

it is now important to look at the possible architectures that could be used in a combined GPS/Galileo E1/L1 receiver.

### POSSIBLE COMMON CBOC/TmBOC TRACKING ARCHITECTURES AND PERFORMANCES

As mentioned in the introductory part, the TmBOC and CBOC modulations, although based on the same two sub-carriers and giving the same PSD, have a very different implementation in the time domain. Consequently, achieving a tracking platform that could be adapted to both modulations is a real challenge.

One of the ideas, investigated in [13] and [16] for CBOC tracking, consisted in the restricted use of pure sub-carriers in order to limit the receiver complexity. Indeed, by doing so, the receiver does not require the use of a multi-bit local replica to track a CBOC signal. Following that idea, two solutions were seen as very promising: the TM61 technique and the dual correlator technique.

#### The TM61 Tracking Technique

This technique was designed to restrict the tracking loop complexity to the lowest possible level, minimizing the number of correlators used. In that context, TM61 is based on the use of Early and Late (E and L) correlations between the incoming CBOC and a pure BOC(6,1) local replica and a Prompt (P) correlation between the incoming CBOC and a pure BOC(1,1). A Dot-Product (DP) discriminator is then formed using these correlators’ outputs. The idea behind is to use the steep BOC(6,1) autocorrelation slope to improve the synchronization (use of E-L) while using the power available in the incoming BOC(1,1) component of the CBOC (use of P) not to suffer from the high BOC(6,1)/CBOC correlation losses. This method is well documented in [13].



It can be shown that under thermal noise TM61 has a performance in terms of equivalent  $C/N_0$  that is 2.5 dBs worse than conventional CBOC tracking, but on the other hand 0.6 dBs better compared to pure BOC(1,1) tracking (assuming an incoming BOC(1,1) signal). This is very interesting because it means that even though the tracking technique is very simple, it still outperforms BOC(1,1) tracking, which was the previous Galileo/GPS E1/L1 baseline modulation for open and civil signals. It was also shown that TM61 was offering an excellent multipath resistance, even better than the one inherent to the CBOC(6,1,1/11) modulation.

### The Dual Correlator Technique

This technique was designed in order to realize two parallel correlations: one between the incoming CBOC and a pure local BOC(1,1) replica and one between the incoming CBOC and a pure local BOC(6,1) replica. The two outputs will be linearly added to form a composite correlator output using the linear property of the correlation operation:

$$\int_0^{T_I} s(t)e_{E1-C}(t) (\rho BOC_{(1,1)}(t) - \beta BOC_{(6,1)}(t)) dt = \quad (14)$$

$$\rho \int_0^{T_I} s(t)e_{E1-C}(t) BOC_{(1,1)}(t) dt - \beta \int_0^{T_I} s(t)e_{E1-C}(t) BOC_{(6,1)}(t) dt$$

This is done for the three E, L, P correlators. As one can recognize, this method poses a slightly higher complexity compared to TM61, but still uses binary local replicas. Initial work was conducted in [16] and proved to be extremely promising.

Indeed, by choosing  $\rho = P$  and  $\beta = Q$ , the dual correlator technique is strictly equivalent to realizing an optimal CBOC correlation. However, by simply changing the respective values of  $\rho$  and  $\beta$ , which can be done in software when forming the discriminator function, it can be expected that more suitable tracking performances can be achieved according to the user priorities.

Changing the values of  $\rho$  and  $\beta$  means, in a strictly equivalent sense, that the incoming CBOC(6,1,1/11) will be tracked using a different local CBOC(6,1,  $\beta^2 / (\rho^2 + \beta^2)$ ). This means that different tracking strategies depending on whether we want to pay more or less attention to the BOC(6,1) component can be used. As an example, as shown in Figure 8 (using the Running Average Multipath Envelope figure of merit), using a local CBOC(6,1,p), with  $p > 1/11$  will help in mitigating multipath better than conventional CBOC(6,1,1/11) tracking because the multipath mitigation capacity of the BOC(6,1) is higher than that of the BOC(1,1) modulation. However, if  $p$  is chosen too high, this might also degrade significantly the resistance of the code tracking loop to thermal noise (due to the high correlation losses). For CBOC(6,1,1/11, '-') tracking, [16]

recommends to use a ratio  $\rho/\beta$  between 1.6 and 3.2 to

have a good compromise between multipath rejection and tracking in white noise (these two values correspond to a local CBOC(6,1,p, '-') with  $p = 4/11$  and  $p = 1/11$  respectively). The corresponding equivalent CBOC local replicas are shown in Figure 7.

It is also possible, if a specific local CBOC waveform is found to fulfill the receiver manufacturer needs, to directly generate locally the CBOC waveform of interest.

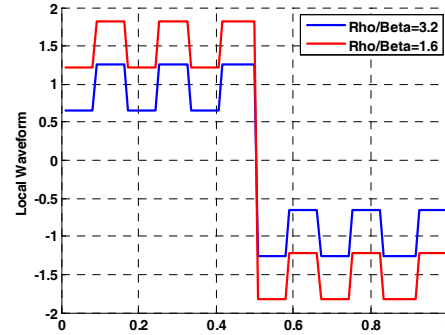


Figure 7. Examples of Equivalent CBOC Local Replicas to Track an Incoming CBOC(6,1,1/11) Signal Using the Dual Correlator Technique

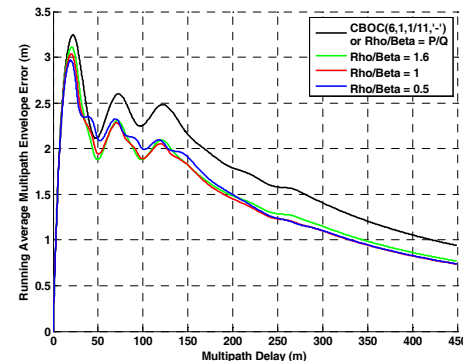


Figure 8. Dual correlator CBOC Multipath mitigation capability for different  $\rho/\beta$  values

In any case, it is suggested that, if a DP discriminator is used, the prompt correlator tries to gather as much useful power as possible since it is responsible for controlling the squaring losses.

### TMBOC Tracking

The correlation degradation, assuming perfect synchronization and an infinite front-end bandwidth, between the TMBOC and a pure BOC(1,1) or BOC(6,1) replica is given by:

$$\text{deg}_{BOC(1,1)/TMBOC(6,1,4/33)} = \frac{29}{33} R_{BOC(1,1)}(0) \approx 0.88 \quad (15)$$

$$\text{deg}_{BOC(6,1)/TMBOC(6,1,4/33)} = \frac{4}{33} R_{BOC(6,1)}(0) \approx 0.12 \quad (16)$$

Comparatively, the same degradation with an incoming CBOC(6,1,1/11) is:

$$\text{deg}_{BOC(1,1)/CBOC(6,1,1/11, '-')} = \sqrt{\frac{10}{11}} R_{BOC(1,1)}(0) \approx 0.95 \quad (17)$$

$$\text{deg}_{\text{BOC}(6,1)/\text{CBOC}(6,1,1/11, \cdot)} = \sqrt{10/11} R_{\text{BOC}(6,1)}(0) \approx 0.3 \quad (18)$$

The consequence is that the degradation is significantly stronger for the TmBOC modulation. In particular, the loss suffered from the TmBOC/BOC(6,1) component is too high to hope using the TM61 tracking technique. In the same way, it can be expected that the dual correlator method will be strongly degraded.

Assuming, for instance, that the BOC(6,1)/TmBOC correlation is of interest, a well-known method against the aforementioned phenomenon is to generate locally a replica composed of the time-multiplexing of 0s where the BOC(1,1) sub-carrier is used in the incoming TmBOC and a BOC(6,1) sub-carrier the rest of the time. The same can be done for the BOC(1,1)/TmBOC correlation. This strongly reduces the correlation losses and puts them at the same level as the CBOC case.

The resulting effect of using these time-multiplexed sub-carriers (BOC(1,1) with 0s and BOC(6,1) with 0s) is that both the TM61 and the dual-correlator methods become relevant. In this case, the TM61 tracking technique applied to TmBOC leads to performances very similar to those obtained with the CBOC(6,1,1/11, ·) (actually 0.2 dBs better in tracking and approximately the same multipath mitigation capability).

The analysis of the dual correlator method is very interesting. Figure 9 shows the code tracking error variance degradation when using the dual correlator technique receiving a TmBOC(6,1,4/33) for different values of  $\rho/\beta$  and assuming an infinite front-end filter. It

can be seen that optimal tracking is obtained for  $\rho/\beta = 1$ , which is normal since this correspond to an equivalent local TmBOC(6,1,4/33) sub-carrier. It can also be seen that there is a small window below that optimal  $\rho/\beta$  value where the tracking degradation is smaller than 0.5 dB. Choosing a value in this interesting window means a potential improvement of the multipath mitigation capability while not significantly reducing the code tracking error due to white noise.

To fully analyze the transposition of the TM61 and dual correlator tracking techniques to TmBOC, it is important to underline certain limitations of that transposition:

- For the TM61 technique, the use of a local replica that is a time-multiplexed signal made of a pure sub-carrier and 0s results in only a partial correlation since not all the spreading code chips are used. This could degrade the cross-correlation properties of the spreading codes. Although it might not be significant for the BOC(1,1) part (it has to be reminded that in this case there are still 29/33 of 10230 chips that are used), it might be detrimental for

the BOC(6,1) part. This is less of a problem for the dual correlator method since a TmBOC signal is recomposed after the linear summation, although because of the different recompositions there might be some losses of cross-correlation properties.

- It might not be interesting, for TmBOC tracking, to replace the use of a local TmBOC replica by a local replica that is a time-multiplexing of a pure sub-carrier with 0s. Indeed, the gain in receiver complexity in this case is not as significant as for the CBOC case. Still, when looking at the dual correlation method, it might be interesting to have the possibility to modify the value of  $\rho/\beta$  on-the-fly.

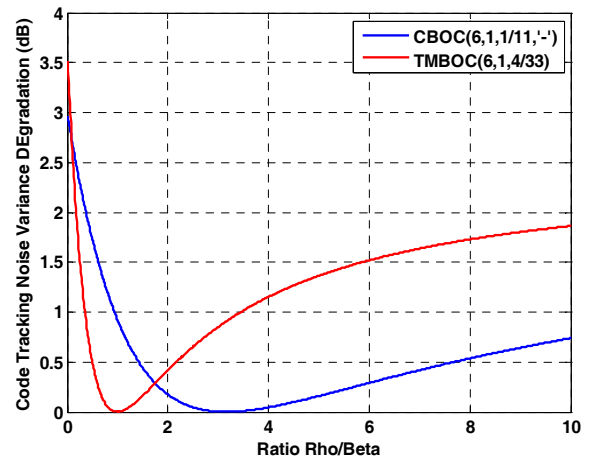


**Figure 9. Code tracking degradation as a function of  $\rho/\beta$  using the dual correlator approach**

### HRC ARCHITECTURE AGAINST MULTIPATH

The previous section looked, among other things, at the impact of multipath on different CBOC/TmBOC tracking techniques. When looking at the global approach against multipath, it is reasonable to investigate if well-known methods that were designed for the GPS C/A code can be easily adapted for CBOC and TmBOC tracking. A typical example of such multipath mitigation technique is the High Resolution Correlator (HRC) presented in [17]. The HRC uses 5 correlators (E2, E, P, L, L2) located at  $[-2d, -d, 0, d, 2d]$  chips where  $2d$  is the E-L spacing. The synthesized HRC E and L correlators can then be synthesized as:

$$\begin{aligned} E_{HRC}(\tau) &= 2E - (E2 + P) \\ L_{HRC}(\tau) &= 2L - (L2 + P) \\ E_{HRC}(\tau) - L_{HRC}(\tau) &= 2(E - L) - (E2 - L2) \end{aligned} \quad (19)$$

Figure 10 shows the multipath envelope associated to the use of the HRC method with a BOC(1,1) receiver receiving a BOC(1,1) signal, a CBOC(6,1,1/11, ·)

receiver receiving a CBOC(6,1,1/11,'-') signal, and a BOC(1,1) receiver receiving a CBOC(6,1,1/11,'-') signal.

It can be seen that the CBOC modulation does not seem to be very well adapted for the use of the HRC. Indeed, many bumps can be observed on the multipath error envelope, while these bumps are not present for the case of the BOC(1,1) signal. We can also recognize that to mitigate multipath with an incoming CBOC signal, the use of a BOC(1,1) receiver with HRC performs better than a CBOC receiver with HRC.

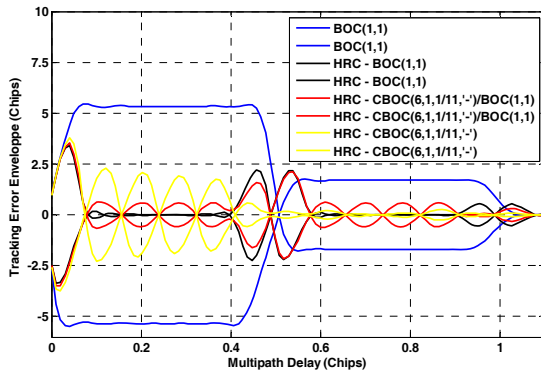


**Figure 10 – Comparison of Multipath Envelope using HRC Applied to BOC(1,1), CBOC and TM61 with  $d=0.08$  chips and a 24 MHz Front-End Filter**

This implies that a different tracking technique will have to be developed for the CBOC and TMBOC signals in order to achieve a multipath mitigation equivalent to that of GPS C/A code when the HRC is used. One way to achieve this is to use more than 5 correlators in order to synthesize a discriminator function that would achieve a desired multipath rejection. This is the scope of the following section.

### OPTIMUM S-CURVE SHAPING OF THE DIFFERENT MBOC IMPLEMENTATIONS

In 2005 a new method to derive an optimum discriminator against code multipath mitigation was presented in [14] using a multi-correlator receiver. At that time, that work was applied to BPSK(1) and BOC(1,1) signals. In 2007, further work has been realized with the convenient modifications to take into account the different MBOC implementations. Detailed information on this multipath mitigation techniques is available in [15].

In [15] two different approaches are discussed. We will concentrate on the first of the two in this paper. This is a conventional tracking loop structure where multiple correlators are employed. The coherent code phase discriminator is defined as a linear combination of the correlators output as follows:

$$\tilde{D}(\Delta\tau) = \sum_{i=1}^N \alpha_i R_i(\Delta\tau) \quad (20)$$

where  $\Delta\tau$  is the code tracking error, defined as the difference between the estimated code delay and the true code delay, and  $\alpha_i$  is the weight of each correlator. Furthermore,  $R_i(\Delta\tau)$  is defined as:

$$R_i(\Delta\tau) = \frac{A}{2} R(\Delta\tau + d_i^{OFF}) e^{j(\varphi_{sat} - \varphi_{rec})} \quad (21)$$

This represents the band-limited autocorrelation function shifted by  $d_i^{OFF}$ . Finally, define the discriminator parameters so as  $d_i^{OFF}$  and  $\alpha_i$  to be properly chosen for each correlator.

The idea behind this work is first to define an ideal S-curve. The optimization process then consists in finding the parameters  $d_i^{OFF}$  and  $\alpha_i$  for a given signal and a given receiver front-end bandwidth that would result in an S-curve fitting with the desired one.

The typical characteristics of an ideal S-curve are:

1. A wide linearity range around 0,
2. An Unambiguous Tracking Offset (UTO) value that results in no false tracking lock point
3. A High-Cut S-Curve (HCS) value

The ideal S-Curve used in the optimization work is depicted in Figure 11.

As shown in figure 11, the introduction of the UTO value results in an S-Curve that has a non-zero value in the outside linear region. Note that this value, expressed in chips, is very little and has a different sign on the two sides of the S-Curve. The main reason to introduce this offset is that by doing so the code discriminator will have only one stable tracking point in the pull-in region. With respect to the HCS, as evident in figure 11, it limits the maximum and minimum values of the S-Curve. The price that we have to pay by introducing these two modifications is that we slightly deviate from the ideal, but the advantages in terms of performance brought by them reward by far this decision.

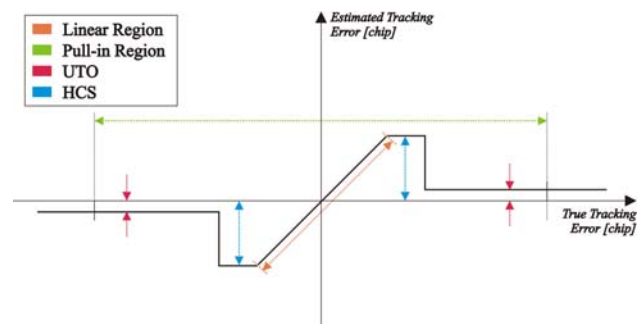


**Figure 11. Optimum S-Curve**

The fitting process consists in approaching the ideal S-Curve by a linear combination of shifted replicas of the autocorrelation function. It can be initiated after defining the number of correlators and their location  $d_i^{OFF}$  within a predefined fitting range and with a certain resolution. The weights  $\alpha_i$  are then calculated, as done in [14], by minimizing the following cost function

$$\sum [\tilde{D}(\Delta\tau) - \tilde{D}_{ID}(\Delta\tau)]^2 \quad (22)$$

where  $\tilde{D}_{ID}$  is the ideal coherent code phase discriminator.

In [15] a realization of the introduced optimum code discriminator has been found for the four different MBOC implementations (CBOC Data and Pilot Channels and TBOC Data and Pilot Channels) at two different values of bandwidth (14 MHz and 24 MHz). For each bandwidth value, a common optimum value of the resolution has been calculated for all the given signals and is presented in Table 6.

**Table 3. Common Optimum Code for MBOC Signals: main parameters**

	14 MHz	24 MHz
Resolution [chip]	0.038	0.028
Extension of S-Curve [chip]	0.05	0.05
UTO [chip]	0.025	0.035
HCS [chip]	0.01	0.01

Two examples of the obtained fitted S-Curve are shown in Figure 12 and Figure 13.

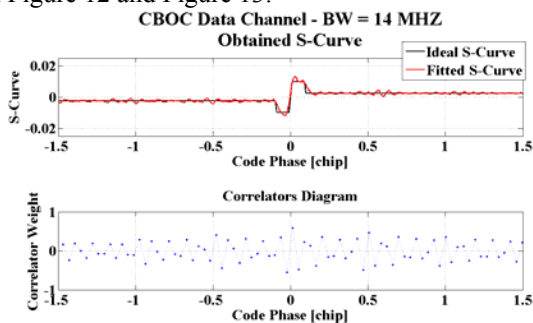


**Figure 12. Example of obtained S-Curve**

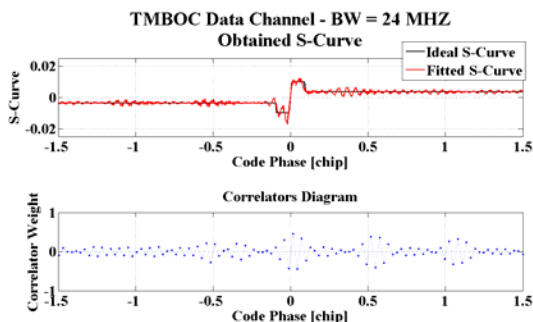


**Figure 13. Example of obtained S-Curve**

It can be seen that in both cases, the resulting discriminator output follows very well the ideal S-curve.

Obviously a large number of correlators are necessary. However, similar results have also been obtained for all the other signals of interest not represented in the previous figures. The results for relatively short bandwidth are particularly impressive. In Figures 14 and 15 the obtained multipath envelopes are depicted.

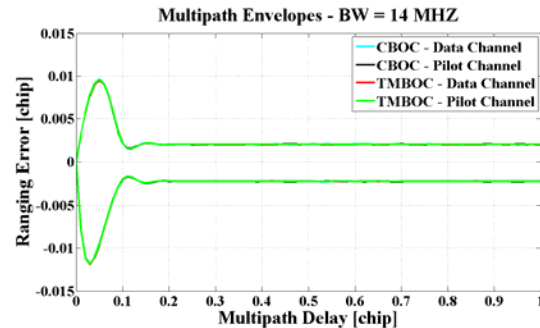


**Figure 14. Multipath Envelopes for a bandwidth of 14 MHz**

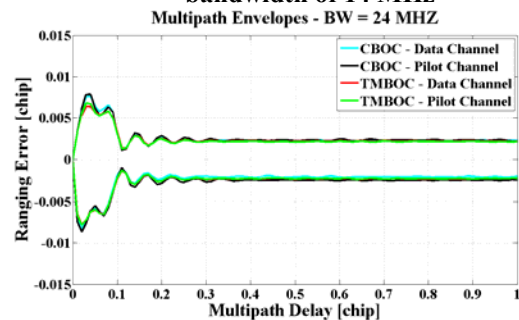


**Figure 15. Multipath Envelopes for a bandwidth of 24 MHz**

It is important to underline that in both cases the multipath envelopes of the four analyzed signal are almost the same. This seems to be a clear sign that the values of the resolution that have been found for each value of bandwidth seem to be “optimal”, in the sense that the performance does not change when the studied signal differs.

## CONCLUSIONS

The first paper has shown that the self-interference between the future Galileo E1 OS and GPS L1C, given their spreading codes and signal structure, will not bring a significant degradation. Moreover, the use of ideal smooth PSD envelopes is a relevant way to estimate their relative SSCs.

The second part was dedicated to the investigation of two simple tracking techniques proposed to track both GPS L1C and Galileo E1 OS pilot channels. The first method, referred to as TM61 represents an ultra simple method to reduce the receiver complexity to a minimum while maintaining interesting performances in terms of CBOC tracking in white noise and multipath. It has been shown that this method only uses pure binary sub-carriers thus avoiding the local generation of a 4-level CBOC replica.

It has also been shown that the adaptation of TM61 for the TBOC requires a more complex local sub-carrier and some associated problems such as the loss of some cross-correlation properties that have to be further investigated.

The second method, the dual correlator tracking technique, uses twice as many correlators as the TM61, realizing once again correlations only between the incoming signal and pure sub-carriers (BOC(1,1) and BOC(6,1) separately). It can achieve optimal tracking performance against both thermal noise and multipath. It can also be easily configured in software to suit a particular user requirement (for instance if multipath is the main problem, if low  $C/N_0$  are expected, or if there is an interference located on the BOC(6,1) part). Once again, the use of this method for CBOC is easier compared than for TBOC for which slight modifications are required in the form of the use of a time-multiplexed sub-carrier. Still it was shown to provide an extremely promising technique.

Finally, in the last part of this paper, it was shown that a simple multipath mitigation technique commonly used in current GPS C/A receivers such as the HRC technique might not be optimal for CBOC or TBOC tracking. However, another technique, based on the optimal use of multi-correlator outputs, was shown to provide excellent multipath mitigation capability for both MBOC implementations, pending a more complex receiver (but that should not be problematic in the long term when multi-correlator receivers could be the baseline).

#### ACKNOWLEDGEMENTS

The authors from FAF University, Munich, wish to acknowledge the financial support for this work by the German Aerospace Center – Deutsches Zentrum für Luft- und Raumfahrt (DLR).

#### REFERENCES

[1] [http://useu.usmission.gov/Dossiers/Galileo\\_GPS/Jul2607\\_Civil\\_Signal\\_Accord.asp](http://useu.usmission.gov/Dossiers/Galileo_GPS/Jul2607_Civil_Signal_Accord.asp)  
 [2] <http://europa.eu/rapid/pressReleasesAction.do?reference=IP/07/1180&format=HTML&aged=0&language=EN&guiLanguage=fr>  
 [3] **Avila-Rodriguez, J.A., G.W. Hein, S. Wallner, J.-L. Issler, L. Ries, L. Lestarquit, A. de Latour, J. Godet, F. Bastide, A.R. Pratt and J. Owen** (2007), *The MBOC Modulation: The Final Touch to the Galileo Frequency and Signal Plan*, Proceedings of the ION-GNSS 2007 (25-28 September, Fort Worth, TX, USA).

[4] **J.A., Avila-Rodriguez** (2007), *On Optimized Signal Waveforms for GNSS*, Ph.D. Thesis, University FAF Munich, Neubiberg, Germany (awaiting publication)

[5] **Hein, G.W., J.-A. Avila-Rodriguez, S. Wallner, A.R. Pratt, J.I.R. Owen, J.-L. Issler, J.W. Betz, C.J. Hegarty, Lt L.S. Lenahan, J.J. Rushanan, A.L. Kraay, and T.A. Stansell** (2006), *MBOC: The New Optimized Spreading Modulation Recommended for GALILEO L1 OS and GPS L1C*, Proceedings of IEEE/ION PLANS (24-27 April, San Diego, CA, USA).

[6] **Hein, G.W., J.-A. Avila-Rodriguez, L. Ries, L. Lestarquit, J.-L. Issler, J. Godet, A.R. Pratt** (2005): *A Candidate for the Galileo L1 OS Optimized Signal*, Proceedings of the ION-GNSS (13-16 September, 2005, Long Beach, CA, USA).

[7] Draft IS-GPS-800 Navstar GPS Space Segment/User Segment L1C Interfaces, 19 April 2006.

[8] **Rushanan, J. J.** (2007) *The Spreading and Overlay Codes for the L1C Signal*, Navigation, the Journal of the ION, Vol. 54, No. 1, pp 43-51

[9] **Raghavan, S., K. Tsai and L. Cooper** (2004), *GPS CDMA Noise Analysis*, AIAA-2004-3182 22<sup>nd</sup> AIAA International Communications Satellite Systems Conference and Exhibit 2004 (ICSSC), (May 9-12, Monterey, CA, USA)

[10] **Kumar, R., S.H. Raghavan, M. Zeitzew, P. Munjal and S. Lazar** (1999) *Analysis of Code Cross Correlation Noise in GPS Receivers Operating in Augmented GPS Systems*, Proceedings of the ION-NTM (Jan. San Diego, CA, USA).

[11] **Raghavan, S., R. Kumar, S. Lazar, M. Zeitzew, R. Wong, J. Michaelson, A. Doran, and M. Bottjer** (1999), *The CDMA Limits of C/A Codes in GPS Applications - Analysis and Laboratory Test Results*, Proceedings of the ION-GNSS 1999 (14-17 Sept., Nashville, TN, USA), pp. 569-580.

[12] **Wallner, S., G.W. Hein, J.-A. Avila Rodriguez, T. Pany, and A. Posfay** (2005), *Interference Computations Between GPS and Galileo*, Proceedings of the ION-GNSS (13-16 Sept., Long Beach, CA, USA).

[13] **Julien, O., C. Macabiau, J.-L. Issler, and L. Ries** (2006), *1-bit Processing of Composite BOC (CBOC) Signals*, 1<sup>st</sup> ESA-CNES workshop on GNSS signals (Toulouse, France)

[14] **Pany, T., M. Irsigler, and B. Eissfeller** (2005), *S-Curve Shaping: A New Method for Optimum Discriminator Based Code Multipath Mitigation*, Proceedings of the ION-GNSS (13-16 Sept., Long Beach, CA, USA).

[15] **Paonni, M., J.-A. Avila-Rodriguez, T. Pany, G.W. Hein, and B. Eissfeller** (2007) *Looking for an Optimum S-Curve Shaping of the Different MBOC Implementations*, Proceedings of the ION-GNSS (25-28 September, 2007, Fort Worth, TX, USA).

[16] **Julien, O., C. Macabiau, J-L. Issler, and L. Ries** (2007) *1-Bit Processing of Composite BOC (CBOC) Signals and Extension to Time-Multiplexed BOC (TMBOC) Signals*, Proceedings of the ION NTM (San Diego, CA, USA)

[17] **Mc Graw, G, and M. Braash** (1999), *GNSS Multipath Mitigation Using Gated and High Resolution Correlator Concept*, Proceedings of the US Institute of Navigation NTM (San Diego, CA, Jan. 25-27), pp. 333-342